J. Non-Newtonian Fluid Mech. xxx (2008) xxx–xxx

Contents lists available at ScienceDirect

Journal of Non-Newtonian Fluid Mechanics

journal homepage: www.elsevier.com/locate/jnnfm

Weakly nonlinear viscoplastic convection

Neil J. Balmforth[a,b], Alison C. Rust[c,*]

[a] Department of Mathematics, University of British Columbia, Vancouver, Canada
[b] Department of Earth and Ocean Science, University of British Columbia, Vancouver, Canada
[c] Department of Earth Sciences, University of Bristol, Bristol, UK

ARTICLE INFO

Article history:
Received 2 April 2008
Received in revised form 11 July 2008
Accepted 19 July 2008
Available online xxx

Keywords:
Viscoplastic fluids
Convection
Yield stress

ABSTRACT

The development of thermal convection is studied for a viscoplastic fluid. If the viscosity is finite at zero shear rate, the critical Rayleigh number for linear instability takes the value given by a Newtonian fluid with that viscosity. The subsequent weakly nonlinear behaviour depends on the degree of shear thinning: with moderate shear thinning, convective overturning for a given temperature difference is amplified relative to the Newtonian case. If the reduction in viscosity is sufficiently sharp the transition becomes subcritical (the relevant situation for many regularized constitutive laws). For an infinite viscosity at zero shear rate, or a yield-stress, the critical Rayleigh number for linear instability is infinite. Nonlinear convective overturning, however, is still possible; we trace out how the finite-amplitude solution branches develop from their Newtonian counterparts as the yield stress is increased from zero for the Bingham fluid. Laboratory experiments with a layer of Carbopol fluid heated from below confirm that yield strength inhibits convection but a sufficiently strong perturbation can initiate overturning.

1. Introduction

Thermal convection of viscoplastic fluids is important in many industrial and geophysical applications. Perhaps the most familiar example is the heating of porridge: "If porridge is cooked in a single saucepan and not stirred it will burn at the bottom. It can still be poured – it is still liquid, but at a certain stage of stickiness convection currents can be prevented even when the bottom is some hundreds of degrees hotter than the top." [1].[1] Jeffreys attributed the lack of convection solely to high viscosity, but porridge is viscoplastic [4] and its non-Newtonian rheology seems to be important for suppressing convection. Although he did not recognize any application to porridge, Jeffreys [3] and several other geophysicists contemplating the thermal convection of the Earth's mantle, were among the first to appreciate that a finite "strength" of a fluid would have substantial effects on convection [5–7]. Orowan [7] showed particular insight remarking that thermal convection would not readily initiate if the fluid has a finite yield stress, but the Newtonian solution is a reasonable approximation once convection is underway.

The onset of thermal convection in a layer of Newtonian fluid confined between plates maintained at different temperatures (the Rayleigh–Bénard problem) is a classic model of instability theory and pattern formation. Indeed, the development of weakly nonlinear theory for the problem [8] laid part of the foundation for the modern theory of dynamical systems. Our goal in the current article is to map out a corresponding analysis for viscoplastic fluid convection. Though one might at first sight imagine this to be straightforward, details of the constitutive model can significantly complicate the situation.

More specifically, a crucial detail of instabilities in viscoplastic fluids is the impact of the yield stress: when patterns develop from a motionless background state, as in the Rayleigh–Bénard problem, that equilibrium is always linearly stable because the yield stress can only be overcome by a finite perturbation (*cf.* [9]). Yet, as also remarked by Orowan, it seems reasonable that the nonlinear convective state is not substantially affected by the yield stress, especially when it is small. A similar situation arises for generalized Newtonian fluids without a yield stress if the viscosity diverges at zero shear rate, as for a shear-thinning power-law fluid.

In Section 2, we develop the weakly nonlinear theory. We approach the problem by treating non-Newtonian effects as small. This allows us to begin a perturbation expansion from the weakly nonlinear Newtonian convection solution. We thereby build the small non-Newtonian effects into the weakly nonlinear model at the same stage of the expansion as the tuned linear instability and nonlinear saturation (the key effects in the Newtonian problem [8]). Importantly, this signifies that we perturb from a fully yielded

* Corresponding author.
E-mail address: Alison.Rust@bristol.ac.uk (A.C. Rust).

[1] Rumford [2] actually initiated the scientific study of thermal convection with a recount of his bowl of rice porridge that after an hour on a stove became cold on top but hot enough at the bottom to burn his mouth. As a result early articles often referred to thermal convection as "the porridge problem" [3].

0377-0257/$ – see front matter © 2008 Elsevier B.V. All rights reserved.
doi:10.1016/j.jnnfm.2008.07.012

convective state and we do not therefore have to face issues regarding the breakup of the rigid plug characterizing the motionless conductive equilibrium. Métivier et al. [10] propose an alternative approach which adds a background shear flow.

The tools developed in Section 2 allow us to draw some general conclusions regarding the effect of shear thinning on convection for generalized Newtonian fluids without a yield stress (Section 3). We restore the yield stress and describe detailed results for the Bingham fluid in Section 4, and compare the weakly nonlinear results with computations of the fully nonlinear steady convective states, which also extends the solutions to higher amplitude and further from the Newtonian limit. Section 5 deals with some analytical solutions to the problem in the limit of short horizontal scale, and Section 6 reconsiders Orowan's "plastic convection". We also describe some laboratory experiments on the initiation of thermal convection in Carbopol (Section 7). We conclude by discussing some industrial and geological applications.

2. Weakly viscoplastic and nonlinear convection

2.1. Formulation

Our goal in this section is to detail a weakly nonlinear theory for a mildly viscoplastic fluid. With that in mind, we consider an incompressible, two-dimensional, Boussinesq fluid layer confined between two horizontal plates held at different temperatures and characterized by some (constant) kinematic viscosity, ν_0. The precise choice of this viscosity will become clear later, but for now its introduction allows us to develop weakly nonlinear theory as for a Newtonian fluid, and add non-Newtonian effects as a perturbation. The configuration is described by a cartesian coordinate system (x, z) in which z points upwards.

As in the conventional development of the Newtonian problem, the equations of motion are expressed conveniently in a dimensionless form, using the depth of the fluid layer, d, in combination with the thermal conductivity, κ, to build units for length, speed and time, and the temperature difference across the plates, $T_1 - T_2$, to measure temperatures (where T_1 and T_2 denote the temperatues of the lower and upper plates, respectively). In terms of a streamfunction, $\psi(x, z, t)$, describing the velocity field, $(u, w) = (-\psi_z, \psi_x)$, and a temperature perturbation, $\theta(x, z, t)$, the equations are

$$\frac{1}{\sigma}[\nabla^2\psi_t + J(\psi, \nabla^2\psi)] = \nabla^4\psi + R\theta_x + N \tag{1}$$

$$\theta_t + J(\psi, \theta) = \nabla^2\theta + \psi_x, \tag{2}$$

where $J(f, g) = f_x g_z - f_z g_x$ and

$$\sigma = \frac{\nu_0}{\kappa} \quad \text{and} \quad R = \frac{g\alpha(T_1 - T_2)d^3}{\nu_0\kappa} \tag{3}$$

are the usual Prandtl number and Rayleigh number, with g being gravity, and α the thermal expansion coefficient. The t, x and z subscripts denote partial derivatives; we depart from this notation only when considering the components of the stresses.

The quantity N originates from the non-Newtonian part of the fluid stresses. More specifically, we denote the *dimensional* deviatoric stress tensor by

$$\tau = \rho\nu_0\left[\frac{\kappa}{d^2}\begin{pmatrix} 2u_x & u_z + w_x \\ u_z + w_x & 2w_z \end{pmatrix} + \breve{\tau}\right], \tag{4}$$

which separates the characteristic viscous stresses from the *dimensionless* non-Newtonian components, $\breve{\tau}$ (scaled by $\rho\nu_0$). Then,

$$N = \frac{\partial^2\breve{\tau}_{xz}}{\partial x^2} - \frac{\partial^2\breve{\tau}_{xz}}{\partial z^2} - 2\frac{\partial^2\breve{\tau}_{xx}}{\partial x\partial z}. \tag{5}$$

Note that we therefore assume that the motionless conduction state is not pre-stressed in any way (so the stress τ has no background component). To allow us analytical inroads into the problem, we solve the equations subject to periodic boundary conditions in x and stress-free, impermeable conditions on the plates: $\psi = \psi_{zz} = 0$ on $z = 0$ and 1. No slip conditions, $\psi = \psi_z = 0$, are potentially more natural, but do not lead to analytical results. However, weakly nonlinear theory can still be applied to that problem, yielding the amplitude equation we derive shortly, but with coefficients that require numerical evaluation.

2.2. Asymptotic expansion

We find a weakly nonlinear solution of the problem by introducing a small parameter $\varepsilon \ll 1$, together with the asymptotic scalings and sequences,

$$\frac{\partial}{\partial t} = \varepsilon^2\frac{\partial}{\partial T}, \qquad R = R_c + \varepsilon^2 R_2, \qquad N = \varepsilon^3 N_3, \tag{6}$$

and

$$\psi = \varepsilon\psi_1 + \varepsilon^2\psi_2 + \varepsilon^3\psi_3 + \ldots, \quad \theta = \varepsilon\theta_1 + \varepsilon^2\theta_2 + \varepsilon^3\theta_3 + \ldots \tag{7}$$

The critical Rayleigh number, R_c, characterizes the onset of convection. The final relation in (6) amounts to a distinguished scaling in which the non-Newtonian effects are tuned to enter the expansion at a certain order, enabling a convenient evaluation of their effect. How the distinguished scaling can be achieved will be described later, when we consider some constitutive laws explicitly.

Via the usual asymptotic machinations, we isolate the terms of equal order in ε, and solve the resulting hierarchy of equations sequentially. At $O(\varepsilon)$,

$$\nabla^4\psi_1 + R_c\theta_{1x} = 0 \tag{8}$$

$$\nabla^2\theta_1 + \psi_{1x} = 0, \tag{9}$$

which have the solution,

$$\psi_1 = A\,\sin(kx + \varpi)\sin\pi z,$$

$$\theta_1 = \frac{\pi k^2 A}{2(\pi^2 + k^2)}\,\cos(kx + \varpi)\sin\pi z, \tag{10}$$

where $A(T)$ and $\varpi(T)$ are not yet determined. For the very onset of convection, we should take $k = \pi/\sqrt{2}$ and $R_c = 27\pi^4/4$, which corresponds to the normal mode that first becomes unstable in the Newtonian problem [8]. However, the weakly nonlinear analysis applies to modes with any horizontal wavelength so we avoid this selection of k, except in considering specific examples. The critical Rayleigh number is then $R_c = (\pi^2 + k^2)^3/k^2$.

At next order, we find

$$\nabla^4\psi_2 + R_c\theta_{2x} = \frac{1}{\sigma}J(\psi_1, \nabla^2\psi_1) = 0 \tag{11}$$

and

$$\nabla^2\theta_2 + \psi_{2x} = J(\psi_1, \theta_1) = \frac{\pi k^2 A^2}{2(\pi^2 + k^2)}\,\sin 2\pi z, \tag{12}$$

which can be solved with

$$\psi_2 = 0, \qquad \theta_2 = -\frac{k^2 A^2}{8\pi(\pi^2 + k^2)}\,\sin 2\pi z. \tag{13}$$

At $O(\varepsilon^3)$,

$$\nabla^4\psi_3 + R_c\theta_{3x} = \frac{1}{\sigma}\nabla^2\psi_{1T} - N_3 - R_2\theta_{1x} \tag{14}$$

$$\nabla^2\theta_3 + \psi_{3x} = \theta_{1T} + J(\psi_1, \theta_2), \tag{15}$$

Please cite this article in press as: N.J. Balmforth, A.C. Rust, Weakly nonlinear viscoplastic convection, J. Non-Newtonian Fluid Mech. (2008), doi:10.1016/j.jnnfm.2008.07.012

or

$$\nabla^6\psi_3 - R_c\psi_{3xx} = (1+\sigma^{-1})\nabla^4\psi_{1T} + R_2\psi_{1xx} - R_c\psi_{1xx}\theta_{2z} - \nabla^2 N_3. \quad (16)$$

The solution requires the satisfaction of the solvability conditions, $\varpi_T = 0$ and

$$(1+\sigma^{-1})\frac{(\pi^2+k^2)^2}{k^2}A_T = R_2 A - \frac{1}{8}(\pi^2+k^2)^2A^3 - \frac{4}{k^2}(\pi^2+k^2)\langle N_3 \sin(kx+\varpi)\sin\pi z\rangle, \quad (17)$$

where the angular brackets denote the integral average over the domain, $0 < kx < 2\pi$ and $0 < z < 1$. Eq. (17) is the desired amplitude equation; without the non-Newtonian effects and for $k = \pi/\sqrt{2}$, it predicts the supercritical onset of steady nonlinear states with $R^2 = 9\pi^2A^2/16$ (*e.g.* [8]). The final term is the non-Newtonian contribution, which has been brought into the amplitude equation at this order via the distinguished scaling, $N = \varepsilon^3 N_3$. Had we chosen a larger scaling, the non-Newtonian effect would have dominated the combination of linear instability and nonlinear saturation.

3. Shear-thinning effects

Consider now a generalized Newtonian fluid with the nonlinear viscosity,

$$\nu = \nu(\dot\gamma), \quad \dot\gamma = \sqrt{4u_x^2 + (u_z+w_x)^2} = \sqrt{4\psi_{xz}^2 + (\psi_{zz}-\psi_{xx})^2}. \quad (18)$$

We focus on onset and take $k = \pi/\sqrt{2}$, implying that, to leading order,

$$\dot\gamma \to \frac{3\pi^3\varepsilon|A|}{2\sqrt{2}}\sqrt{8\,\cos^2(kx+\varpi)\cos^2\pi z + \sin^2(kx+\varpi)\sin^2\pi z} \equiv \varepsilon\dot\gamma_1. \quad (19)$$

Thus, we identify the characteristic scale $\nu_0 = \nu(0)$, and then the Taylor expansion of the viscosity law is $\nu = \nu_0 + \nu'(0)\dot\gamma + (1/2)\nu''(0)\dot\gamma^2 + \ldots$ Thence,

$$N \equiv \left(\frac{\partial^2}{\partial x^2} - \frac{\partial^2}{\partial z^2}\right)\left[\left(\frac{\nu}{\nu_0}-1\right)(\psi_{xx}-\psi_{zz})\right] + 4\frac{\partial^2}{\partial z\partial x}\left[\left(\frac{\nu}{\nu_0}-1\right)\psi_{xz}\right]. \quad (20)$$

Note that in writing the equation above, we must assume that $\nu'(0)$ is finite and that we can adjust the size of the coefficients $\nu'(0)$ and $\nu''(0)$ as needed to ensure that $N = O(\varepsilon^3)$. However, many constitutive models such as the power-law fluid have $\nu_0 = 0$ and $\nu'(0) \to \infty$. It is well appreciated that such behaviour is unphysical and a regularization procedure applied to limit the viscosity. The resulting regularized model can then be analyzed as follows. Otherwise, one must proceed down a similar avenue to that used for the Bingham model in Section 4. (It is more difficult to perturb off a Newtonian fluid for constitutive models like the power-law fluid.)

3.1. $\nu'(0) = 0$

If $\nu'(0) = 0$, we may write

$$\frac{\nu}{\nu_0} - 1 \to -\varepsilon^2\nu_2\dot\gamma_1^2, \quad (21)$$

where $\nu_2 = -\nu''(0)/2\nu_0$, with the sign included to reflect shear thinning. The non-Newtonian term, N, automatically turns out to be order ε^3, and performing the needed integrals in the amplitude equation (17) gives,

$$(1+\sigma^{-1})\frac{9\pi^2}{2}A_T = R_2 A - \frac{9\pi^2}{32}A^3\left(1 - \frac{601\pi^4\nu_2}{12}\right). \quad (22)$$

Thus, the weakly nonlinear branch that bifurcates from the conduction state at the critical Rayleigh number is

$$R_2 = \frac{9\pi^2}{32}A^2\left(1 - \frac{601\pi^4\nu_2}{12}\right). \quad (23)$$

For a given Rayleigh number (temperature difference), shear thinning therefore counterbalances the suppression of the mean temperature gradient (the main Newtonian nonlinear effect) and allows the unstable mode to grow to greater amplitude. Indeed, if ν_2 is sufficiently large, the right-hand side of Eq. (23) becomes negative, reflecting how the nonlinear solution appears at lower Rayleigh numbers than the critical value. In other words, sufficient shear thinning can make the transition to instability subcritical.

3.2. $\nu'(0) \neq 0$

If $\nu'(0) \neq 0$, we take $\nu'(0)/\nu_0 = -\varepsilon\nu_1$, to ensure that $N = O(\varepsilon^3)$. The non-Newtonian contribution can be evaluated to give an amplitude equation with the form,

$$(1+\sigma^{-1})\frac{9\pi^2}{2}A_T = R_2 A + \Gamma A^2\ \mathrm{sgn}(A) - \frac{9\pi^2}{32}A^3\left(1 - \frac{601\pi^4\nu_2}{12}\right), \quad (24)$$

where Γ is a positive numerical constant proportional to ν_1. The nonlinear steady branch is then

$$R_2 = \frac{9\pi^2}{32}A^3\left(1 - \frac{601\pi^4\nu_2}{12}\right) - \Gamma|A|. \quad (25)$$

Sufficiently close to the bifurcation, the viscosity correction embodied in Γ dominates the nonlinear terms and generates a subcritical transition. Provided $1 > 601\pi^4\nu_2/12$, the branch subsequently turns around in a saddle-node bifurcation and becomes a stable nonlinear branch. Sketches summarizing the results for $\nu'(0) = 0$ and $\nu'(0) \neq 0$ are illustrated in Fig. 1.

3.3. Regularized constitutive laws

Regularized viscoplastic constitutive laws typically have the feature of replacing a singular character at zero shear rate with a Newtonian, but strongly viscous, behaviour. In this situation, one can identify the characteristic scale ν_0 as the regularized, zero-shear-rate viscosity, and this viscosity dictates the linear instability threshold. However, by definition, the constitutive law should be extremely shear thinning in order to capture a sudden switch to the unregularized viscoplastic model. Our results above then indicate that the transition to instability must become subcritical.

For example, a possible regularization of the Bingham model is incorporated in the law,

$$\tau = \rho\nu_p\left[1 + \frac{B}{(\delta^m + \dot\gamma^m)^{1/m}}\right]\dot\gamma, \quad (26)$$

where ν_p is the equivalent plastic viscosity, m and $\delta \ll 1$ are positive parameters (with $\varepsilon \ll \delta$ so as not to violate the ordering of the asymptotic expansion of Section 2) and

$$B = \frac{\tau_y d^2}{\rho\nu_p\kappa}$$

Please cite this article in press as: N.J. Balmforth, A.C. Rust, Weakly nonlinear viscoplastic convection, J. Non-Newtonian Fluid Mech. (2008), doi:10.1016/j.jnnfm.2008.07.012

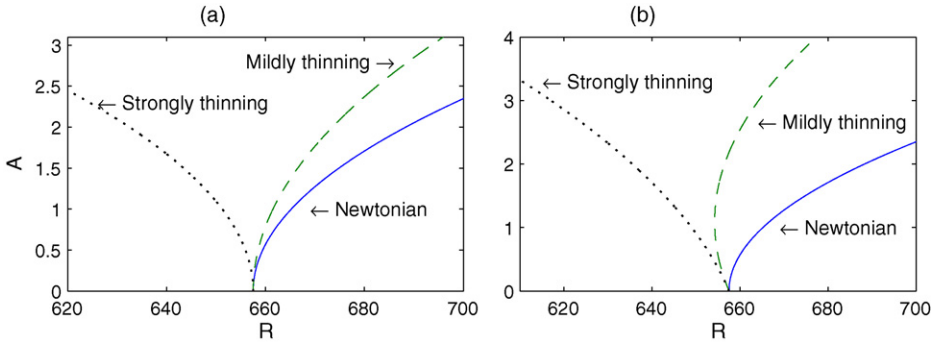

Fig. 1. Sketches of the bifurcating branches of steady convection for a Newtonian fluid and a shear-thinning material with (a) $\nu'(0)=0$ and (b) $\nu'(0)\neq 0$. In each case, two non-Newtonian examples are given (labelled "mildly" and "strongly" thinning), showing the two possible behaviours.

is equivalent to a Bingham number based on the large shear rate, effective yield stress, τ_y. We may define

$$\nu_0 \equiv \nu_p\left(1+\frac{B}{\delta}\right) \gg \nu_p,$$

as the characteristic viscosity, which therefore gives a critical Rayleigh number much higher than that for a Newtonian fluid with viscosity ν_p. (Alternatively we may keep ν_p as the characteristic viscosity, in which case, B/δ must be taken $O(\varepsilon^3)$, as done explicitly in the next section.)

For $m=2$, $\nu'(0)=0$ and the viscosity law Taylor expands to give

$$\nu_2 \equiv \frac{1}{2\delta(B+\delta)} \approx \frac{1}{2\delta B} \gg 1. \tag{27}$$

This factor easily overcomes the suppression of the mean temperature gradient to reverse the criticality of the transition to instability.

If $m=1$ on the other hand,

$$\frac{\nu'(0)}{\nu_0} \equiv -\frac{B}{\delta(B+\delta)}, \tag{28}$$

which can be tuned to be order ε by taking $B=O(\varepsilon)$. Thus, either way, the transition becomes subcritical, as illustrated by the "strongly thinning" cases of Fig. 1. Note that the popular Papanastasiou [11] regularization gives similar results to Eq. (28), but with ν_1 proportional to the "stress growth parameter".

The regularizations discussed above assume a strongly viscous low-shear-rate behaviour. However, materials such as Carbopol also display significant elasticity in this regime. A viscoelastic regularization of the Bingham model actually allows for the possibility of an oscillatory type of convective instability. In Appendix A we show that this instability is unlikely in practice.

4. The Bingham model

4.1. Weakly nonlinear results

For the Bingham model, with plastic viscosity, ν_0, and yield stress, τ_y,

$$\tau = \left(\rho\nu_0 + \frac{\tau_y}{\dot\gamma}\right)\dot\gamma, \quad \text{if } \tau_y < \sqrt{\frac{\tau_{jk}^2}{2}}, \tag{29}$$

we have

$$\breve\tau = B\frac{\dot\gamma}{\dot\gamma}, \tag{30}$$

where the Bingham number is again $B=\tau_y d^2/(\rho\kappa\nu_0)$. To ensure that $N=O(\varepsilon^3)$, we therefore take $B=\varepsilon^3 B_3$.

Eq. (29) applies when the fluid is yielded; otherwise, we set $\dot\gamma = \sqrt{\dot\gamma_{jk}^2/2}=0$. The perturbation analysis assumes that the perturbed state remains fully yielded. Indeed, it is straightforward to show that, for the Newtonian normal mode, $\dot\gamma=0$ only at distinct points. However, it is conceivable that unyielded plugs develop about those points when the yield stress is introduced. We return to this issue below when we describe some fully nonlinear computations (see also [9]); for now, we assume that the development of any plugs does not affect the accuracy of the perturbation theory.

With this assumption, we perform the integral describing the non-Newtonian contribution in the amplitude equation (17):

$$(1+\sigma^{-1})\frac{(\pi^2+k^2)^2}{k^2}A_T = R_2 A - \frac{1}{8}(\pi^2+k^2)^2A^3 - B_3\Gamma\,\mathrm{sgn}(A), \tag{31}$$

where

$$\Gamma \equiv \frac{4}{k^2}(\pi^2+k^2) \times \left\langle \sqrt{4\pi^2k^2\,\cos^2 kx\cos^2\pi z+(\pi^2-k^2)^2\sin^2 kx\sin^2\pi z}\right\rangle \tag{32}$$

$$\approx 78.32 \quad \text{if } k=\frac{\pi}{\sqrt{2}}. \tag{33}$$

Note that, if $A=0$, we should interpret $\mathrm{sgn}(A)=0$, which allows for the conduction equilibrium solution in this equation.

The steady finite-amplitude solutions are now given implicitly by

$$R_2 = \frac{1}{8}(\pi^2+k^2)^2A^2 + \frac{B_3\Gamma}{|A|}. \tag{34}$$

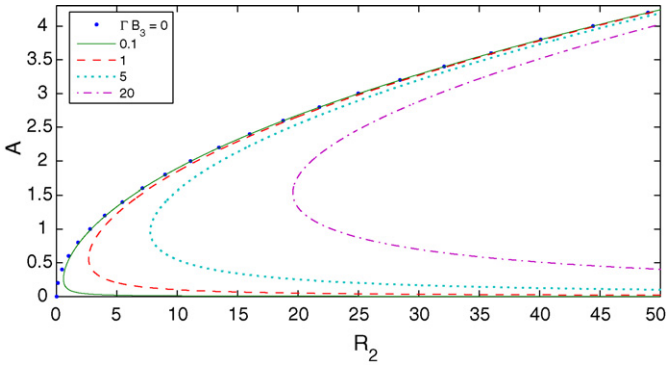

Fig. 2. Steady solutions to the amplitude equation (31) for varying values of ΓB_3 (as marked). Only the solutions with positive A are shown—the corresponding solution branches with $A<0$, are obtained by reflection about the R_2-axis.

Please cite this article in press as: N.J. Balmforth, A.C. Rust, Weakly nonlinear viscoplastic convection, J. Non-Newtonian Fluid Mech. (2008), doi:10.1016/j.jnnfm.2008.07.012

Importantly, there is no longer any connection between the finite-amplitude branches and the conduction state ($A=0$). Instead, the remnant of the stable nonlinear solution turns around in a saddle-node bifurcation near the Newtonian linear onset, and proceeds off to $(R_2, A)\to(\infty,0)$ as an unstable nonlinear solution branch (Fig. 2).

The saddle-node occurs for

$$A=\left[\frac{4B_3\Gamma}{(\pi^2+k^2)^2}\right]^{1/3} \quad \text{and} \quad R_2=\frac{3}{2}\left[\frac{1}{2}B_3\Gamma(\pi^2+k^2)\right]^{2/3}. \tag{35}$$

The lower, *unstable* solution branch also has the asymptote,

$$|A|\to\frac{\Gamma B_3}{R_2}, \tag{36}$$

for large R_2. In the simple dynamical system, in addition to determining the amplitude of the unstable mode, this is also the threshold to which the mode amplitude must be kicked in order to observe a transition to finite-amplitude convection on the stable branch.

4.2. Numerical results

To complement the weakly nonlinear theory, we solve the steady versions of Eqs. (1) and (2) numerically using the truncated Fourier series,

$$\psi=\sum_{j=1}^{J}\sum_{n=1}^{N}[A_{nj}^{(1)}\sin(2j-1)kx\ \sin(2n-1)\pi z+A_{nj}^{(2)}\ \sin 2jkx\ \sin 2n\pi z], \tag{37}$$

$$\theta=\sum_{j=1}^{J}\sum_{n=1}^{N}[B_{nj}^{(1)}\cos(2j-1)kx\ \sin(2n-1)\pi z + B_{nj}^{(2)}\ \cos 2(j-1)kx\ \sin 2n\pi z], \tag{38}$$

which preserve the Boussinesq symmetry. Projection of the governing equations onto each Fourier mode generates a system of nonlinear algebraic equations that we solve by Newton iteration, starting with guesses guided by the weakly nonlinear theory or existing solutions. For simplicity, we take $\sigma\to\infty$, which removes the nonlinear advection terms from the momentum equations.

Results for $B=0$ and 1 are shown in Fig. 3, which displays the bifurcated branches of nonlinear overturning states on the (R, A)-plane, where the amplitude, $A=A_{11}^{(1)}$ (*i.e.* the first modal coefficient in the Fourier expansion of ψ). Except at the highest mode amplitudes, the weakly nonlinear theory matches the nonlinear computations.

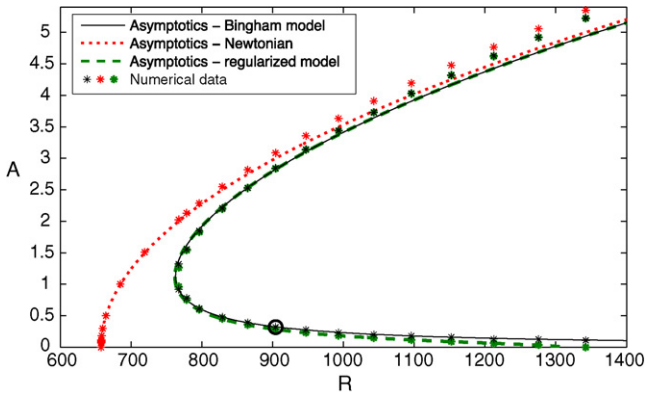

Fig. 3. Amplitudes of nonlinear overturning states, defined as $A=A_{11}^{(1)}$ (the first modal in the Fourier expansion of ψ). The solid (dotted) line shows the weakly nonlinear result for $B=1$ ($B=0$). The dashed lines shows the corresponding asymptotic result for the regularized model (26) with $B=\delta=1$ and $m=2$, but derived in the limit $B=O(\varepsilon^3)$ and $\delta=O(\varepsilon)$. The points show the results of numerical computations taking $N=J=16$ and $\sigma\to\infty$. The circle indicates the solution of Fig. 5.

To connect the current analysis with Section 3, we also include in Fig. 3 results for the regularized model (26) with $m=2$. The weakly nonlinear results assume $B=O(\varepsilon^3)$ and $\delta=O(\varepsilon)$ in the regularization, so the non-Newtonian contribution to the amplitude equation (17) can be written as

$$12A^{-1}B_3\langle\dot\gamma_1^2(\delta^2+\dot\gamma_1^2)^{-1/2}\rangle. \tag{39}$$

For large amplitude, this contribution becomes small and we recover the Newtonian solution, but for $A\to0$, the regularized viscosity dominates to give a linear damping term that corrects the critical Rayleigh number. The results in Fig. 3 are computed with the somewhat larger value, $\delta=1$, but the weakly nonlinear predictions nevertheless match the numerical computations.

Two planforms of nonlinear solutions are illustrated in Figs. 4 and 5. These pictures show a solution along the upper branch of stable nonlinear states, and one along the unstable lower branch, respectively. In both cases, the plots of the total deformation rate, $\dot\gamma$, suggest that small plug regions may develop near the boundaries and middle of the layer (the former being allowed by the stress-free boundary conditions). These regions are not particularly well captured by our numerical scheme and cause the Fourier series to converge slowly. Indeed, to improve the convergence, it is helpful to include the regularization described above (but with $\delta=10^{-3}$ or so, which assists the convergence by suppressing the tails of the spectra, whilst not overly smoothing the solutions). Nevetheless, the plugs remain localized near onset and do not appear to influence the accuracy of the weakly nonlinear results. Further from onset, extensive plug regions can develop, as

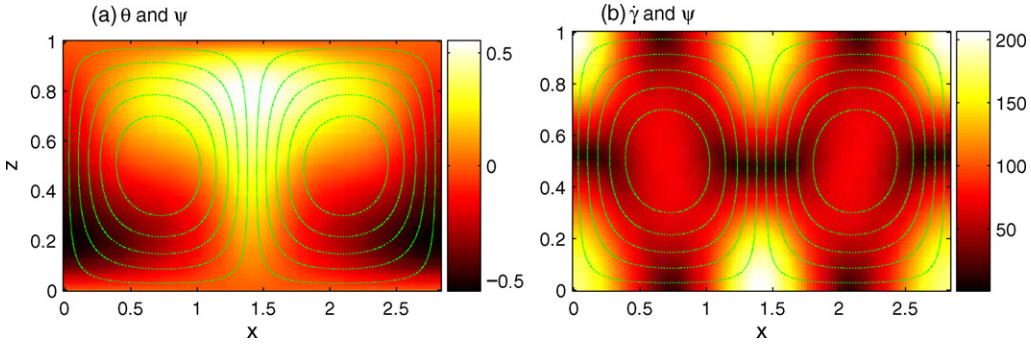

Fig. 4. Numerical solution for $B=1$ and $R=5.1667R_c$ along the upper branch of nonlinear overturning states. Panels (a) and (b) show the temperature perturbation, θ, and shear rate, $\dot\gamma$, as densities on the (x, z)-plane. The dotted contours indicate the streamfunction, ψ.

Please cite this article in press as: N.J. Balmforth, A.C. Rust, Weakly nonlinear viscoplastic convection, J. Non-Newtonian Fluid Mech. (2008), doi:10.1016/j.jnnfm.2008.07.012

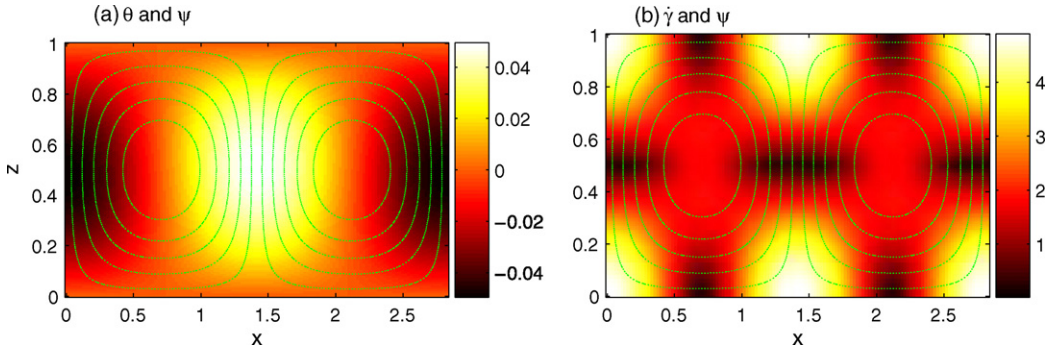

Fig. 5. Numerical solution for $B = 1$ and $R = 1.375R_c$ along the lower branch of nonlinear overturning states. The panels are as represented in Fig. 4.

illustrated by the short wavelength patterns described in the next section.

5. Short-wavelength patterns

5.1. Vertically localized rolls

The nonlinear solutions constructed above have $k = \pi/\sqrt{2}$, in line with the most unstable modes of the Newtonian problem. We now depart from that choice of wavelength and illustrate a family of solutions with short horizontal scale which can be constructed analytically: As illustrated in Fig. 6, in the limit of $k \gg 1$, the numerical solutions become dominated by a single horizontal wavenumber and occupy a localized, yielded region centred in the fluid layer. Above and below this layer, the fluid is unyielded and stagnant. As shown in Appendix B (and illustrated in Fig. 6), these layered solutions are approximately given by

$$\psi = \Psi(z)\,\cos kx, \tag{40}$$

with

$$\Psi(z) = \begin{cases} \dfrac{4}{3\pi} BM^{-2}\left[1+\cos M\left(z-\dfrac{1}{2}\right)\right], & \left|z-\dfrac{1}{2}\right| \le \pi M^{-1} \\ 0, & \text{elsewhere} \end{cases} \tag{41}$$

and

$$M = \sqrt{\frac{R-k^4}{3k^2}}. \tag{42}$$

which are valid for $R \sim k^4$ and $M \sim k$ ($R_c \approx k^4$ for $k \gg 1$).

5.2. Viscoplastic elevators

A second analytically accessible family of solutions are the periodic arrays of "elevators" considered by Gershuni & Zhukhovitskii [12] which are the z-independent solutions to (1) and (2) for an infinitely deep layer. The fluid yields and shears in localized zones separated by uniformly ascending and descending plugs. The elevator system is illustrated in Fig. 7, and, in the current notation, can be described as follows. If we centre one of the sheared zones at $x = 0$, the streamfunction there is

$$\psi = A\left(\frac{\cos mkx}{\cos m\Sigma} + \frac{\cosh mkx}{\cosh m\Sigma}\right) \quad \text{for} \quad -\Sigma \le kx \le \Sigma, \tag{43}$$

and the plugs bordering this zone are given by

$$\psi = 2A\left[\frac{(\pi/2)-kx}{\Sigma-(\pi/2)}\right], \qquad \text{over} \quad \Sigma < |kx| < \pi - \Sigma. \tag{44}$$

Here, $m = R^{1/4}/k$, and the scaled half-width of the sheared region, Σ, is given implicitly by the relation,

$$2 = m\left(\frac{\pi}{2} - \Sigma\right)(\tan m\Sigma - \tanh m\Sigma). \tag{45}$$

The amplitude, A, is determined from

$$A = \frac{k^2 B}{R}\,\frac{m}{(\pi/2)-\Sigma}\left[\frac{2}{3}m\left(\frac{\pi}{2}-\Sigma\right) + \tan m\Sigma + \tanh m\Sigma\right]^{-1}. \tag{46}$$

Fig. 7 shows how Σ and A vary with m. Note that $(\Sigma,\ RA/k^2B) \to (\pi/2,\ 1/2)$ as $m \to 1$ (the onset of convection in the Newtonian version of the problem), and $(\Sigma, RA/k^2B) \to ((6/\pi)^{-1/3}m^{-4/3}, 6/\pi^2)$

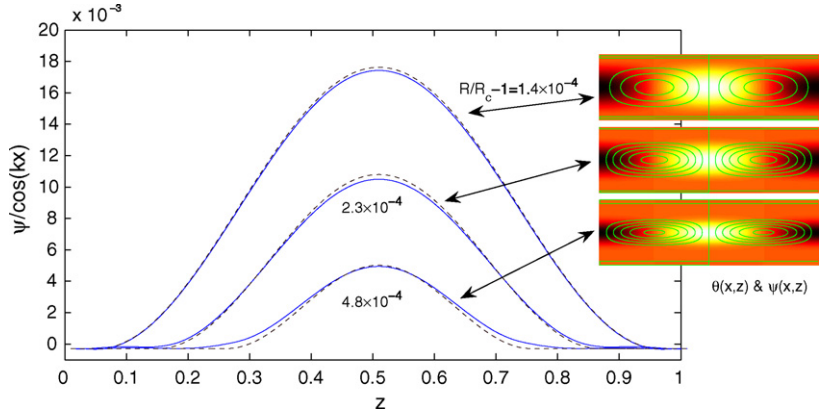

Fig. 6. Short-wavelength, layered solutions for $k = 1000$ and three values of R (as indicated); $B = 1$. The regularization, $\delta = 0.01$, has been included to help compute the solutions. The main panel shows the streamfunction, ψ, divided by $\cos kx$, at 10 positions in x to emphasize how the solution is dominated by a single wavenumber. The dashed lines show the asymptotic result in (41). The insets show plots of the corresponding temperature perturbations, $\theta(x, z)$, as densities on the (x, z)-plane, with superimposed streamlines.

Please cite this article in press as: N.J. Balmforth, A.C. Rust, Weakly nonlinear viscoplastic convection, J. Non-Newtonian Fluid Mech. (2008), doi:10.1016/j.jnnfm.2008.07.012

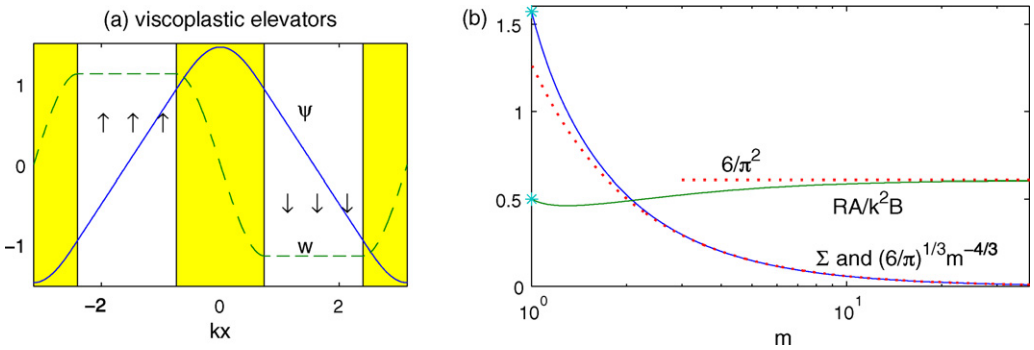

Fig. 7. Viscoplastic elevator solutions. Panel (a) shows part of a sample elevator system, with the shaded region indicating the yielded zones, the dashed line showing w, and the solid curve showing ψ (as given by (43)–(46), with $m = 1.6$ and $\Sigma = \pi/4$). Panel (b) shows the solutions to (45) and (46) for Σ and RA/k^2B as functions of m. The solutions for Newtonian case and for $m \to \infty$ are shown with starts and dotted lines, respectively.

as $m \to \infty$. Also, the combinations, $m^4 = R/k^4$, $k^2\ B/R$ and kx, are all independent of the layer depth, d, for a fixed background temperature gradient, $(T_1 - T_2)/d$. Thus, the solution does not depend on that lengthscale (as must be the case) and the problem could be scaled differently at the outset.

Although the elevator solutions appear irrelevant for a layer of finite thickness, it is conceivable that these solutions may form the basis of roll solutions with boundary layers adjacent to the bounding plates (though we have been unable to verify this numerically).

6. Scalings and plastic convection

The results presented above indicate that, although strongly unstable convective systems might be linearly stable, there is a finite amplitude instability. Moreover, the threshold in amplitude above which the system must be kicked to initiate convection becomes increasingly lower as the Rayleigh number increases. Once convection begins, yield stresses become less significant and the convective states likely resemble the Newtonian counterparts.

The results further suggest that there are unstable steady states whose amplitude in ψ or θ scale like B/R (Table 1). The amplitude scaling also incorporates an additional geometrical factor which allows for the possibility that the solutions become spatially localized, with convective cells separated by rigid plugs. Though it is not guaranteed, it seems plausible that the amplitude of these steady states furnishes an estimate of the threshold for finite-amplitude instability (as in the weakly nonlinear theory). The dimensionless amplitude threshold can then be written as

$$\frac{B}{R} = \frac{\tau_y}{\rho g \alpha (T_2 - T_1) d}, \tag{47}$$

which can be viewed alternatively as the ratio of yield stress to buoyancy. Thus, for example, the introduction of a perturbation with an associated temperature perturbation of order $\tau_y/(\rho g \alpha d)$, ought to be sufficient to initiate convection.

Note that the asymptotic scaling, $(\psi, \theta) \sim B/R$, of the low-amplitude unstable solutions also suggests a limiting behaviour for $R \to \infty$ described by the system,

$$\theta_x + R^{-1}N = \nabla^2\theta + \psi_x = 0, \tag{48}$$

which was previously considered by Orowan [7] for thermal convection in a perfectly plastic medium. Orowan suggested that this type of convection was realized physically, whereas here we see that this is unlikely given that the solutions are unstable.

Table 1
Estimates of amplitudes of stable branches

Model	Amplitude
Weakly nonlinear (Section 4.1)	$\Gamma B/R \approx (78B/R)$ if $k = k_c = \pi\sqrt{2}$
Layered solution (Section 5.1)	$8k^2B/\pi R$
Viscoplastic elevators (Section 5.2)	$12k^2B/\pi^2R$

7. Qualitative laboratory experiments

To test the notion that the yield stress replaces a supercritical transition at finite Rayleigh number with a subcritical threshold, we conducted a set of preliminary experiments with Carbopol 940 in a rectangular tank. The tank consists of four glass walls, each 30 cm wide, bonded with silicone sealant to the top of a hollow metal box, which could be heated to temperatures up to 80 °C by a hot water circulation system. The tank was partially filled with Carbopol to a depth (d) between 4 and 11 cm. After a transient, the basal temperature (T_1) was held constant; however, the temperature at the top of the Carbopol (T_2) was not controlled and gradually warmed up from room temperature. Temperatures at several points within the fluid were monitored with thermocouples, and temperature perturbations at the top surface were seen as colours on a temperature-sensitive liquid–crystal-coated polyester sheet floating atop the Carbopol.

Four concentrations of Carbopol were used: 0.05, 0.06, 0.075 and 0.1 wt.% dry Carbopol dispersed in distilled water and neutralized with NaOH. The density and thermal properties are essentially the same as for pure water, and the viscosity and apparent yield strength variations with temperature are small compared to variations with shear rate and Carbopol concentration. Estimates of yield stress based on 1°, 4 cm diameter cone-and-plate rheometry, and the sinking of spheres of different sizes and densities [13] are given in Table 2.

The different concentrations of Carbopol showed marked differences in their ability to convect: Experiments where 0.05% Carbopol ($\tau_y < 0.1$ Pa; Table 2) was heated from below lead to convection without imposing any external trigger. The ratio of yield stress to buoyancy (B/R) is very low for this concentration, and the rise of a few air bubbles, slight lateral variations in temperature, or other external vibrations might easily be responsible for overcoming the threshold for convection. Indeed, we estimate that temperature fluctuations of less than 1 °C are necessary to initiate convection in this fluid (see the final column of Table 2, which estimates the threshold described in Section 6).

By contrast, none of the other concentrations spontaneously began to convect if left undisturbed. For the range of fluid depths

Please cite this article in press as: N.J. Balmforth, A.C. Rust, Weakly nonlinear viscoplastic convection, J. Non-Newtonian Fluid Mech. (2008), doi:10.1016/j.jnnfm.2008.07.012

Table 2
Summary of conditions and results for a subset of the experiments

Carbopol (wt.%)	τ_y (Pa)	d (m)	$T_1 - T_2$ (°C)	Convects?	B/R	$\tau_y/(\rho g\alpha d)$ (°C)
0.05	<0.1	0.044	27	Yes	<0.04	<1
0.05	<0.1	0.113	36	Yes	<0.01	<0.4
0.06	0.3	0.1	50	No/Yes*	0.03	1.5
0.075	2	0.1	50	No	0.2	10
0.1	10	0.1	50	No	1	49

The two 0.05 wt.% Carbopol experiments quote the temperature difference recorded at the onset of convection, whereas the temperature differences for the three other experiments are the maxima imposed. The lengthscale d is used where necessary, which underestimates the characteristic perturbation amplitude of the final column, $\tau_y/(\rho g\alpha d)$ (see Section 6), if the relevant lengthscale is actually the growing boundary-layer thickness rather than d. The * indicates when tank-scale convection was only initiated with a major perturbation.

and temperature limits described above, convection was only initiated with the 0.06% Carbopol ($\tau_y \approx 0.3$ Pa) if the system was substantially perturbed by methods such as injecting large air bubbles at the base, or mixing up a column of fluid in the tank with a stirrer. Attempts to destabilize the 0.075 and 0.1% Carbopol ($\tau_y \approx 2$ and 10 Pa, respectively) by such methods caused only local transient temperature perturbations and did not generate any thermal plumes or tank-scale convection. Thus, the experiments also suggest that yield stress suppresses convection but can be overcome with a sufficient kick to the system. Furthermore, the amplitude of the perturbation required to initiate convection increases with increasing yield strength. Nevertheless, a proper quantitative comparison with the theoretical results of Sections 3 and 4 requires experiments with better controls on the temperature of the top surface.

8. Summary and applications

In this article we have explored how the steady, weakly nonlinear, overturning solutions of the Newtonian Rayleigh–Bénard problem are modified when the fluid is made viscoplastic. Shear thinning amplifies the overturning states for a given temperature difference, and can make the transition to instability subcritical if the degree of thinning is sufficiently large. The introduction of a yield stress suppresses the linear convective instability entirely. Instead, an unstable, subcritical branch of nonlinear convective states bifurcates from infinite Rayleigh number. That branch turns around in a saddle node near the onset of Newtonian convection to generate stable overturning solutions corresponding to the original Newtonian convective states. The theory suggests that the unstable branch has a (dimensionless) amplitude scaling of B/R, which suggests that a temperature perturbation of order $\tau_y/(\rho g\alpha d)$ is necessary to kick the system off the conducting state into finite-amplitude convection.

According to weakly nonlinear theory, the turn-around in the saddle-node occurs at Rayleigh numbers of order $B^{2/3}$, where B is a Bingham number based on the velocity scale, κ/d (Section 3.3). This suggests that stable convective solutions cease to exist when the yield stress becomes as high as

$$\tau_y \sim \frac{\rho[g\alpha(T_2 - T_1)]^{3/2} d^{5/2}}{(\nu_0\kappa)^{1/2}}. \tag{49}$$

In other words, convection is turned off by a sufficiently high yield stress. Nevertheless, two other types of solutions that we have described (viscoplastic elevators and vertically localized rolls) extend down to the Newtonian onset. Though these solutions are unstable, their existence casts some doubt on the estimate in (49).

These results are relevant to understanding and controlling flow and heat transfer in a wide range of industrial and geophysical settings where viscoplastic thermal convection may occur. These include ice slurries in refrigeration systems and around extraterrestrial bodies [14], drilling muds and gels [15,16], various magma bodies [17,18], and mud volcanoes [19]. Although geophysicists interested in convection of the Earth's mantle were amongst the first to consider the effect of yield strength on convection (Section 1), the mantle is now generally thought to have a power-law or Newtonian rheology with significant dependence on temperature and pressure. However, yield strength (with highly viscous or elastic sub-yield-stress deformation) has recently been considered in attempts to explain superficial plate-like behaviour (*e.g.* [20,21]).

Our results suggest that in all of these applications, yield strength will inhibit convection and heat transfer, and that the greater the yield strength, the larger the perturbation required to initiate convection. Furthermore, unlike the Newtonian case, the conditions (temperature difference and lengthscale) required to initiate convection can be quite different from those required to perpetuate convection. This disparity can be particularly important for applications where the fluid rheology could change from Newtonian to viscoplastic with time as is indeed the case with porridge. As another example, we discuss thermal convection of crystal-rich magmas.

Understanding the role of crystals in magma convection has implications for the generation of some types of economic ore deposits [22] as well as volcanic eruption triggers and magma degassing [18,23]. Magmas composed of pure melt (silicate liquid), or melt with dilute suspensions of crystals, are viscous, Newtonian fluids. However, magmas containing substantial volume fractions of crystals are generally considered to be viscoplastic, and the yield strength can be estimated, for instance, from the shapes of lava domes slowly extruded from volcanic vents (*e.g.* [24]). As a magma cools (or in some circumstances decompresses), the crystal content, and thus the viscosity and yield strength, increase [25]. Hence there may be circumstances where crystal-rich magma can continue to convect despite a significant yield strength, because the magma was Newtonian (or had a substantially lower yield strength) when convection began, as might occur in magma chambers beneath volcanoes or in open-channel lava flows [26]. Moreover, for the mobilization of a stagnant layer that is already crystal-rich, it is not sufficient to consider the Newtonian criterion for convection (as done by [23]). In this scenario, yield strength may prevent or substantially delay instability, and convection may be limited to the hotter (less crystalline) portions of the magma chamber.

This picture of magma convection is entirely qualitative. Accurate quantitative predictions of the critical Rayleigh number and perturbation required for onset are not yet feasible in natural systems where the geometry and boundary conditions are not ideal, and rheology varies substantially both spatially and temporally. Even in our more simplistic Carbopol experiments, the changing upper boundary condition precludes quantitative agreement with theory. Before tackling complex natural problems, experiments approximating the ideal conditions of the theory are required.

Acknowledgements

ACR thanks NSERC and the Royal Society of London for support. We thank Mark Jellinek for discussions and use of his laboratory facilities and the referees for their constructive criticisms.

Appendix A. Viscoelastic oscillatory instability

Many viscoplastic fluids, including Carbopol, exhibit viscoelastic behaviour at low stresses [27]. However, the ability of the yield stress to suppress the linear convective instability follows in part because viscoplastic constitutive laws like the Bingham model

Please cite this article in press as: N.J. Balmforth, A.C. Rust, Weakly nonlinear viscoplastic convection, J. Non-Newtonian Fluid Mech. (2008), doi:10.1016/j.jnnfm.2008.07.012

neglect any deformation below the yield stress. If this behaviour is regularized by adding a low-shear-rate viscosity, the critical Rayleigh number becomes finite. This leads one to wonder how the dynamics might be affected by viscoelasticity below the yield stress, as might be important in materials like Carbopol. In this situation, the linear convective instability is controlled by a combination of the viscosity and an elastic relaxation rate. Although the latter does not influence the transition to steady convection, it does lead to the possibility of another type of convective instability in which rolls overturn in an oscillatory fashion [28,29].

A simple Maxwell model provides a concise illustration since for the linear instability calculation, all we need is a linear constitutive law. More specifically, we interpret ν_0 as a solvent-like viscosity, and $\breve{\tau}_{ij}$ as the contribution from some equivalent polymeric (elastic) stresses, with

$$\breve{\tau} + \Lambda \breve{\tau}_t = \mu \dot{\gamma}. \tag{A.1}$$

In this dimensionless equation, the parameters Λ and μ represent, respectively, the ratio of polymer to solvent viscosities and the polymer relaxation time scaled by the diffusion timescale d^2/κ.

On combining this model with the linearized versions of (1) and (2), looking for normal modes of the form, $(\psi,\theta) \propto e^{i\omega t + ikx} \sin n\pi z$, and demanding that ω is purely real, we arrive at the critical conditions,

$$\omega = 0, \qquad R = R_{st} = (1+\mu)\frac{K^6}{k^2} \tag{A.2}$$

or

$$\omega^2 = \frac{\sigma\lambda[(1+\mu)K^6 - k^2 R]}{K^2(K^2+\sigma K^2+\Lambda)},$$

$$R = R_{osc} = \frac{K^2}{k^2}\left(\frac{\Lambda}{\sigma}+K^2\right)\left(K^2+\Lambda+\frac{\mu\sigma\Lambda}{1+\sigma}\right), \tag{A.3}$$

where $K^2 = n^2\pi^2 + k^2$. The onset of steady convection, as given by (A.2), is therefore modified according to the increase in total viscosity (the factor $1+\mu$). Moreover, steady convection can be preceded by the onset of oscillatory convection if the smallest value of the critical Rayleigh number, R_{osc}, in (A.3) over all k lies below the minimum of R_{st}. The most unstable modes for either steady or oscillatory convection have $n = 1$—the tallest vertical modes. The most unstable horizontal wavenumber remains $k = \pi/\sqrt{2}$ for steady convection; the corresponding value of k for oscillations depends on the detailed parameter settings.

For a sub-yield-stress viscoplastic fluid, one envisions that the polymeric stresses are relatively large, so that the material behaves almost like a rigid solid. That is, the parameters μ and Λ should be large. In that limit, onset is given by either

$$R_{c,st} = \mathrm{Min}_k(R_{st}) \to \frac{27\pi^4\mu}{4} \quad \text{and} \quad k = k_c = \frac{\pi}{\sqrt{2}} \tag{A.4}$$

or

$$R_{c,osc} = \mathrm{Min}_k(R_{osc}) \to \frac{\mu\Lambda^2}{1+\sigma} \text{ and } k = k_c \sim \left(\frac{\pi^2\Lambda}{\sigma}\right)^{1/4} \gg 1. \tag{A.5}$$

Thus, the onset of oscillatory convection is unlikely to precede steady convection. In other words, steady convection is favoured if a sub-yield-stress viscoplastic fluid is to behave almost rigidly.

Appendix B. Short-wavelength and low-amplitude layered solutions

To understand the structure of the short-wavelength, low-amplitude, layered solutions, we return to the governing dimensionless equations without the nonlinear advection terms. We introduce another small parameter, $\lambda = k^{-1} \ll 1$, characterizing the relatively short wavelength. We then rescale the horizontal coordinate and perturbations to suit the short scale: $x = \lambda\xi$, $(u,w) = (U(\xi,z), \lambda^{-1}W(\xi,z))$, $p = \lambda^{-1}P(\xi,z)$ and $\theta = \lambda\Theta(\xi,z)$. Moreover, since the short-scale solutions become unstable for $R \sim k^4$, we put $R = \lambda^{-4} + \lambda^{-2}r$. Thence,

$$U_\xi + W_z = 0, \tag{B.1}$$

$$0 = -P_\xi + U_{\xi\xi} + \lambda^2 U_{zz} + \lambda^2\partial_\xi T_{xx} + \lambda^2\partial_z T_{xz}, \tag{B.2}$$

$$0 = -\lambda^2 p_z + (1+\lambda^2 r)\Theta + W_{\xi\xi} + \lambda^2 W_{zz} + \lambda^2\partial_\xi T_{xz} + \lambda^4\partial_z T_{zz}, \tag{B.3}$$

$$0 = \Theta_{\xi\xi} + \lambda^2\Theta_{zz} + W, \tag{B.4}$$

where the yield-stress terms have been rescaled so that $(\breve{\tau}_{xx}, \breve{\tau}_{xz}, \breve{\tau}_{zz}) = (\lambda T_{xx}, T_{xz}, -\lambda T_{xx})$, and

$$T_{xz} = \frac{2BU_\xi}{\sqrt{(W_\xi+\lambda^2 U_z)^2 + 4\lambda^2 U_\xi^2}},$$

$$T_{xz} = \frac{B(W_\xi+\lambda^2 U_z)}{\sqrt{(W_\xi+\lambda^2 U_z)^2 + 4\lambda^2 U_\xi^2}}. \tag{B.5}$$

A standard asymptotic expansion can be used to solve this set of equations: let $U = U_0 + \lambda^2 U_2$, $W = W_0 + \lambda^2 W_2$, and so on. To leading order,

$$p_{0\xi} = U_{0\xi\xi}, \quad 0 = \Theta_0 + W_{0\xi\xi}, \quad 0 = \Theta_{0\xi\xi} + W_0, \quad U_{0\xi} + W_{0z} = 0. \tag{B.6}$$

Thus, the solution is dominated by a single wavenumber:

$$W_0 = \Theta_0 = \Psi(z)\cos\xi, \quad U_0 = -\Psi'(z)\sin\xi, \quad P_0 = -\Psi'(z)\cos\xi. \tag{B.7}$$

Note that, to leading order,

$$T_{xz} \to B\ \mathrm{sgn}(W_{0\xi}) = -B\,\mathrm{sgn}(\Psi\sin\xi). \tag{B.8}$$

The vertical structure function, $\Phi(z)$, follows from considering the order λ^2 equations, and, in particular,

$$W_{2\xi\xi} + \Theta_2 = -(2\Psi'' + r\Psi)\cos\xi + B\partial_\xi[sgn(\Psi\sin\xi)], \tag{B.9}$$

$$\Theta_{2zz} + W_2 = -\Psi''\cos\xi. \tag{B.10}$$

At this stage, the system does not admit a solution that is periodic in ξ unless we apply a solvability condition, obtained on multiplying the relations by $\cos\xi$ and averaging over the horizontal wavelength. This demands that Ψ satisfies the differential equation,

$$3\Psi'' + r\Psi = -\frac{4B}{\pi}\,\mathrm{sgn}(\Psi). \tag{B.11}$$

To match the numerical solutions described in the main text, we solve this equation subject to the boundary conditions that $(\Psi, \Psi') \to 0$ at the edges of the yielded region, which is centered in the layer. This gives the solution quoted in Section 5. The fluid above and below the centered yielded region is held rigid by the yield stress. Although the numerical scheme converges to a solution that is centered in the layer, in principle the asymptotic solution could be off-centered with rigid layers of arbitrarily thickness above and below.

References

[1] H. Jeffreys, The porridge problem, St. John's Coll. Camb. Sir Harold Jeffreys Pap. C17 (1957), http://janus.lib.cam.ac.uk/db/node.xsp?id=EAD%2FGBR%2F0275%2FJeffreys%2FC7-C29.

Please cite this article in press as: N.J. Balmforth, A.C. Rust, Weakly nonlinear viscoplastic convection, J. Non-Newtonian Fluid Mech. (2008), doi:10.1016/j.jnnfm.2008.07.012

[2] B. Thompson, (Count Rumford), The Complete Works of Count Rumford, Vol. I. Of the Propagation of Heat in Fluids. Part I, The American Academy of Arts and Sciences, Boston, 1870.
[3] H. Jeffreys, The Earth, 3rd ed., Cambridge University Press, 1952.
[4] J. Dejongh, J. Steffe, Yield stress of hot cereals by the vane method, J. Text. Stud. 35 (2004) 1–9.
[5] D. Griggs, A theory of mountain building, Am. J. Sci. 237 (1939) 611–650.
[6] F. Vening Meinesz, Major tectonic phenomena and the hypothesis of convection currents in the earth, Q. J. Geol. Soc., Lond. 103 (1948) 191–207.
[7] E. Orowan, Convection in a non-Newtonian mantle, continental drift, and mountain building, Philos. Trans. R. Soc. Lond. Ser. A 258 (1965) 284–313.
[8] W. Malkus, G. Veronis, Finite amplitude cellular convection, J. Fluid Mech. 4 (1958) 225–260.
[9] J. Zhang, D. Vola, I. Frigaard, Yield stress effects on Rayleigh–Bénard convection, J. Fluid Mech. 566 (2006) 389–419.
[10] C. Métivier, C. Nouar, J.-P. Brancher, Linear stability involving the Bingham model when the yield stress approaches zero, Phys. Fluids 17 (2005) 104106.
[11] T. Papanastasiou, Flows of materials with yield, J. Rheol. 31 (1987) 385–404.
[12] G. Gershuni, E. Zhukhovitskii, Convective stability of a Bingham liquid, Sov. Phys. Doklady 18 (1973) 36p.
[13] A.N. Beris, J.A. Tsamopoulos, R.C. Armstrong, R.A. Brown, Creeping motion of a sphere through a Bingham plastic, J. Fluid Mech. 158 (1985) 219–244.
[14] P. Egolf, M. Kauffeld, From physical properties of ice slurries to industrial ice slurry applications, Int. J. Refriger. 28 (2005) 4–12.
[15] E. Santoyo, A. Garcia, G. Espinosa, S. Santoyo-Gutiérrez, E. González-Partida, Convective heat-transfer coefficients of non-Newtonian geothermal drilling fluids, J. Geochem. Expl. 78-79 (2003) 249–255.
[16] Y. Bayazitoglu, P. Paslay, P. Cernocky, Laminar Bingham fluid flow between vertical parallel plates, J. Therm. Sci. 46 (2007) 349–357.
[17] H. Hardee, Convective heat extraction from molten magma, J. Volcanol. Geotherm. Res. 10 (1981) 175–207.
[18] O. Bachmann, G. Bergantz, Gas percolation in upper-crustal silicic crystal mushes as a mechanism for upward heat advection and rejuvenation of near-solidus magma bodies, J. Volcanol. Geotherm. Res. 149 (2006) 85–102.
[19] P. Henry, S.L. Pichon, S. Lallemant, S. Lance, J. Martin, J.-P. Foucher, A. Fiala-Médioni, F. Rostek, N. Guilhaumou, V. Pranal, M. Castrec, Fluid flow in and around a mud volcano field seaward of the Barbados accretionary wedge: results from Manon cruise, J. Geophys. Res. 101 (1996) 20297–20323.
[20] D. Bercovici, The generation of plate tectonics from mantle convection, Earth Planet. Sci. Lett. 205 (2003) 107–121.
[21] D. Turcotte, G. Schubert, Geodynamics, second ed., Cambridge University Press, 2002.
[22] H. Shinohara, J. Hedenquist, Constraints on magma degassing beneath the Far Southeast porphyry Cu–Au deposit, Philippines, J. Petrol. 38 (1997) 1741–1752.
[23] S. Couch, R. Sparks, M. Carroll, Mineral disequilibrium in lavas explained by convective self-mixing in open magma chambers, Nature 411 (2001) 1038–1039.
[24] R. Griffiths, The dynamics of lava flows, Annu. Rev. Fluid Mech. 32 (2000) 477–518.
[25] K. Cashman, C. Thornber, J. Kauahikaua, Cooling and crystallization of lava in open channels, and the transition of pahoehoe lava to ‘a‘a, Bull. Volc. 61 (1999) 306–323.
[26] R. Griffiths, R. Kerr, K. Cashman, Patterns of solidification in channel flows with surface cooling, J. Fluid Mech. 496 (2003) 33–62.
[27] J. Piau, Carbopol gels: elastoviscoplastic and slippery glasses made of individual swollen sponges. Meso- and macroscopic properties, constitutive equations and scaling laws, J. Non-Newton. Fluid Mech. 144 (2007) 1–29.
[28] Z. Li, R. Khayat, Finite-amplitude Rayleigh–Bénard convection and pattern selection for viscoelastic fluids, J. Fluid Mech. 529 (2005) 221–251.
[29] P. Kolodner, Oscillatory convection in viscoelastic DNA suspensions, J. Non-Newton. Fluid Mech. 75 (1998) 167–192.

Please cite this article in press as: N.J. Balmforth, A.C. Rust, Weakly nonlinear viscoplastic convection, J. Non-Newtonian Fluid Mech. (2008), doi:10.1016/j.jnnfm.2008.07.012